The Budgets of Turbulent Kinetic Energy and Temperature Variance in the Atmospheric Surface Layer

J. C. WYNGAARD AND O. R. COTÉ

Air Force Cambridge Research Laboratories, Bedford, Mass.

(Manuscript received 12 August 1970, in revised form 30 November 1970)

ABSTRACT

Measurements of the shear production, buoyant production, turbulent transport (flux divergence) and dissipation terms in the budget of turbulent kinetic energy, and production and turbulent transport terms in the temperature variance budget are presented. Direct observations of the surface stress and heat flux over a horizontally uniform site enable presentation of the data in terms of surface layer similarity theory.

The dissipation term, obtained from differentiated hot-wire anemometer signals, agrees with estimates made from the inertial subrange levels of longitudinal velocity spectra with a value of 0.5 for the spectral constant. Under stable conditions dissipation essentially balances shear production, while turbulent transport and buoyant production are of secondary importance. Under unstable conditions, dissipation slightly exceeds the total production, and energy is also lost at a substantial rate due to upward export by the turbulence.

The large imbalance among the measured terms in the energy budget under unstable conditions is discussed. The cause of the imbalance cannot at this point be determined with certainty, but an interesting possibility is that pressure transport is significant under very unstable conditions.

The production rate of temperature variance exceeds its rate of vertical transport by an order of magnitude. Estimates of the universal temperature spectral constant were made with the assumption that temperature variance dissipation and production rates are equal; the average value, 0.8, falls within the range reported by other workers.

1. Introduction

In the summer of 1968 the Boundary Layer Branch of the Meteorology Laboratory of AFCRL made extensive measurements of wind and temperature in the first 32 m of the atmospheric surface layer. The experiment site was an extremely flat area in southwest Kansas, having 2400 m of uniform wheat stubble to the south, the prevailing wind direction during the experiments. The instrumentation included two drag plates for surface stress measurements, three 3-component sonic anemometers and three platinum resistance thermometers for wind and temperature fluctuations at three levels, three constant-temperature linearized hot-wire anemometers for measurement of the streamwise wind fluctuations to frequencies of 2000 Hz, and cup anemometers and resistance thermometers for measurement of mean wind and temperature profiles.

This experiment has allowed a detailed study of the budgets of turbulent kinetic energy and temperature variance in the surface layer. Previous efforts, summarized by Lumley and Panofsky (1964), have had a number of limitations, so that until now only the rough outlines of the budgets have been drawn. The Kansas experiments were unique in having direct measurements of production, turbulent transport, and dissipation rates of turbulent energy, and the production and transport rates of temperature variance, allowing a quantitative determination of their imbalance over wide range of stability conditions. In addition, the direct flux measurements have allowed the data to be presented in the context of similarity theory (Obukhov, 1946; Monin and Obukhov, 1954), which permits a concise representation of the effects of stability.

2. Instrumentation, data collection and data reduction

The sonic anemometers (Kaijo Denki PAT 311), hot wires (DISA 55D05–55D15) and fast-response thermometers (Cambridge Systems Model 127) were mounted at 5.66, 11.3 and 22.6 m on the tower. Cup anemometers and thermometers for mean profile measurements were placed at 2, 4, 8, 16, 22.6 and 32 m, with cups also at 5.66 and 11.3 m to allow comparison with sonic anemometer speeds. The drag plates were located about 50 m east-southeast of the tower. A detailed description of the site is given by Haugen *et al.* (1971).

Data were digitized and stored on magnetic tape by the computer-controlled data acquisition system described by Kaimal *et al.* (1966). The profile instrumentation was sampled once per second, and the other instruments 20 times per second. The hot-wire outputs were differentiated and low-pass filtered with filters of the type described by Wyngaard and Lumley (1967). This prewhitening process amplified the high-frequency turbulence components before recording on the FM channels of an Ampex FR-1300 tape recorder and

allowed subsequent data analysis out to 2000 Hz, which was sufficient to cover essentially the entire dissipation range.

By comparing the mean speeds of the cup and sonic anemometers, it has been established by Izumi and Barad (1970) that the cup speeds are about 10% high. This is due to the dynamic nonlinearity of the cup anemometer (it reacts differently to wind speed increases and decreases) and to its sensitivity to the fluctuating vertical wind component. Cup anemometer speeds were therefore reduced by 10% for use on wind profiles.

Since obtaining data from hot wires is less straightforward than with the other instruments, a brief discussion will be given here. The wires were 1.2 mm long and were mounted vertically. This length, approximately equal to the Kolmogorov microscale, was sufficiently short so that the attenuation in the mean-square velocity derivatives due to the finite wire length (Wyngaard, 1969) was no more than a few percent.

Absolute calibration of the hot wires in the field was not attempted. Rather, wind tunnel testing was done to assure that the static response curve was indeed linear over the operating range. That is, the output E was related to the longitudinal air speed U by

$$E=a+bU. \tag{1}$$

The fluctuating response was then

$$e=bu. \tag{2}$$

Taylor's hypothesis implies that

$$\frac{\partial e}{\partial t}=-bU\frac{\partial u}{\partial x}. \tag{3}$$

Assuming isotropy, the dissipation rate ϵ is

$$\epsilon=15\nu\overline{\left(\frac{\partial u}{\partial x}\right)^2}=\frac{15\nu}{(E-a)^2}\overline{\left(\frac{\partial e}{\partial t}\right)^2}. \tag{4}$$

To obtain the variance of the derivative of the fluctuating output signal, the recorded derivative signal was reproduced and digitized at ~3000 samples sec^{-1}.

The above expressions for hot-wire response and Taylor's hypothesis are accurate, strictly speaking, only for vanishing turbulence levels. Slight corrections are needed for application in the atmospheric surface layer. For hot-wire response, the expressions derived by Rose (1962) were used. Eq. (1) was replaced by

$$\left.\begin{aligned} E&=a+bS\\ S&=\frac{U}{\left(1-\dfrac{v^2}{2U^2}\right)}\end{aligned}\right\}. \tag{5}$$

The set (5) reflects the fact that the mean hot-wire output is proportional to the mean horizontal wind speed S, and not the mean streamwise wind component U. Eq. (2) becomes

$$e=b\left[u-K_1\theta S+\frac{S}{2}\left(\frac{v^2}{S^2}-\frac{\overline{v^2}}{S^2}\right)\right]. \tag{6}$$

The second term within the bracket represents the sensitivity to temperature fluctuations; K_1 was typically $2.5\times10^{-2}(°C)^{-1}$ in this experiment. The final term corrects for the difference between fluctuations of horizontal speed and streamwise velocity.

The final correction to be made involves Taylor's hypothesis. Heskestad (1965) proposed that in high Reynolds number turbulent shear flow, the higher order terms in the frozen field expression

$$\frac{Du}{Dt}=0=\frac{\partial u}{\partial t}+(U+u)\frac{\partial u}{\partial x}+v\frac{\partial u}{\partial y}+w\frac{\partial u}{\partial z} \tag{7}$$

be retained. By assuming isotropy at small scales and independence of structure at widely varying scales, he showed that

$$\overline{\left(\frac{\partial u}{\partial t}\right)^2}=U^2\overline{\left(\frac{\partial u}{\partial x}\right)^2}\left[1+\frac{\overline{u^2}}{U^2}+\frac{2\overline{v^2}}{U^2}+\frac{2\overline{w^2}}{U^2}\right]. \tag{8}$$

Similar expressions hold for the derivatives of v and w.

The dissipation calculation started with the differentiated form of Eq. (6), which relates $\partial e/\partial t$ and $\partial u/\partial t$. The effects of the temperature and lateral velocity fluctuation terms were found to be negligible. Heskestad's modified Taylor's hypothesis [Eq. (8)] was then used to convert to mean-square streamwise derivatives, with the correction factor typically being 10–20%. Finally, the assumption of isotropy [Eq. (4)] gave dissipation rates from the streamwise derivative variances.

3. The turbulent energy budget

In high Reynolds number atmospheric turbulence, the budget of turbulent kinetic energy per unit mass is expressed by (Lumley and Panofsky, 1964)

$$\frac{1}{2}\frac{\partial\overline{u_iu_i}}{\partial t}+\frac{U_j}{2}\frac{\partial\overline{u_iu_i}}{\partial x_j}+\overline{u_iu_j}\frac{\partial U_i}{\partial x_j}-\frac{g}{T}\overline{\theta u_3}+\frac{1}{2}\frac{\partial\overline{u_iu_iu_j}}{\partial x_j}+\nu\overline{\frac{\partial u_i}{\partial x_j}\frac{\partial u_i}{\partial x_j}}+\frac{1}{\rho}\overline{\frac{\partial pu_i}{\partial x_i}}=0. \tag{9}$$

Here U_i and u_i are the mean and fluctuating parts, respectively, of velocity in the x_i direction, and repeated indices are summed; T and θ are the mean and fluctuating temperature; ρ is the mean density; p the fluctuating

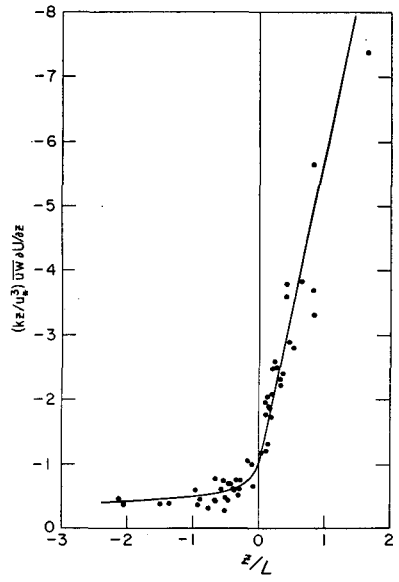

FIG. 1. Dimensionless rate of shear production of energy.

pressure; and g the acceleration of gravity. The subscript notation is convenient for Eq. (9), but in what follows we replace u_i and x_i by (u, v, w) and (x, y, z), respectively.

The energy budget simplifies considerably under horizontally homogeneous conditions, where mean quantities depend only on the vertical coordinate z and the mean velocity has only the streamwise (x) component U. We expect the smallest scales of motion to have an isotropic structure, so the expression for dissipation can also be simplified. The steady-state budget is then

$$\overline{uw}\frac{\partial U}{\partial z}-\frac{g}{T}\overline{w\theta}+\frac{1}{2}\frac{\partial\overline{wq^2}}{\partial z}+15\nu\overline{\left(\frac{\partial u}{\partial x}\right)^2}+\frac{1}{\rho}\frac{\partial\overline{pw}}{\partial z}=0, \quad (10)$$

where $q^2=u^2+v^2+w^2$.

The first four terms in Eq. (10) were measured directly. The first term is the rate of production of energy by the interaction of Reynolds stress with the mean strain rate; we will call this shear production. The second term represents the rate of working against the buoyancy forces; we call this buoyant production, and note that it is a source or a sink depending on the sign of the vertical heat flux. The third term is the divergence of the turbulent flux of kinetic energy, which we will call turbulent transport. The fourth term is the rate of conversion of turbulent energy into internal energy by the action of viscous forces, or simply the dissipation rate. The final term in Eq. (10) is another flux divergence; it represents the transfer of energy from one point in space to another due to the fluctuating pressure, and we call this pressure transport.

The assumption of horizontal homogeneity was primarily responsible for the simplification of the energy budget from Eq. (9) to Eq. (10). Unfortunately, the Kansas experiments included no direct measurements to test this assumption; it may seem reasonable because of the uniform surface conditions and long fetch, but without measurements we cannot be certain. At this point it seems preferable to lump possible inhomogeneity effects together with the pressure transport and call this the imbalance term I. We take therefore as our model of the energy budget

$$\overline{uw}\frac{\partial U}{\partial z}-\frac{g}{T}\overline{w\theta}+\frac{1}{2}\frac{\partial\overline{wq^2}}{\partial z}+15\nu\overline{\left(\frac{\partial u}{\partial x}\right)^2}+I=0. \quad (11)$$

It has long been assumed, and recently demonstrated by Haugen *et al.* (1971), that to a good approximation the surface layer is a "constant flux" layer. That is, the turbulent fluxes $\overline{uw}$ and $\overline{w\theta}$ are effectively independent of height from the surface. For these conditions similarity theory predicts that certain aspects of the turbulent structure are uniquely determined by the parameters $\overline{w\theta}$, $\overline{uw}$, g/T and z. Accordingly, we nondimensionalize the terms in Eq. (11) with kz/u_*^3, where u_*, called the friction velocity, is the square root of the kinematic surface shearing stress, and k is von Kármán's constant. From similarity theory the terms in the budget should be universal functions of z/L, where L, the Obukhov length, is defined by

$$L=\frac{-u_*^3T}{kg\overline{w\theta}}. \quad (12)$$

The friction velocity u_* was derived from the average of the two drag plate readings, as discussed by Haugen *et al.*

Since the observations revealed no significant systematic variation of heat flux with height, the average of the three measured values was used in calculating L. Von Kármán's constant k was taken as 0.35, rather than the usual vales of 0.40, as a result of the profile analysis reported by Businger *et al.* (1971).

We now proceed to a discussion of the behavior of the terms in Eq. (11). The results are presented in dimensionless form, and it should be pointed out that the choice of kz/u_*^3 as a normalizing factor is not critical for the interpretation of the budget. Since all terms are normalized with the same factor, their relative magnitudes are unchanged. In all cases we refer the terms to the left side of Eq. (9), so that if a term represents an energy gain, it is negative.

a. Shear production

Measurements of the dimensionless shear production term are shown in Fig. 1, each point representing a 1-hr run. Reynolds stresses were computed for 15-min blocks of data, and four of these values were averaged to give the stress for the run.

The average properties of this curve should be those of the nondimensional wind shear ϕ_m, where

$$\phi_m = \frac{kz}{u_*}\frac{\partial U}{\partial z}. \tag{13}$$

The observations of ϕ_m from this experiment are presented in Businger *et al.* (1971). The scatter in Fig. 1 is somewhat greater than found in ϕ_m, due to the run-to-run scatter of $-\overline{uw}/u_*^2$ about its average value of 1.0.

From the profile analysis, it has been found that in unstable conditions ϕ_m is represented well by the Businger-Dyer formula

$$\phi_m = (1-15z/L)^{-\frac{1}{4}}. \tag{14}$$

Under stable conditions, the form

$$\phi_m = 1+4.7z/L \tag{15}$$

is a good fit. These interpolation formulas are shown in Fig. 1.

b. Buoyant production

Buoyant production simply normalizes to

$$-\frac{kz}{u_*^3}\frac{g\overline{w\theta}}{T} = \frac{z}{L}, \tag{16}$$

and is therefore a gain under unstable conditions and a loss during stable conditions.

c. Turbulent transport

Hourly estimates of turbulent transport were made by approximating the vertical derivative of $\overline{wq^2}$. Its value was available at the three sonic levels, and we used

$$\frac{kz}{u_*^3}\frac{\partial(\overline{wq^2}/2)}{\partial z} = \frac{k\partial\overline{wq^2}}{u_*^3\partial(2\ln z)} \approx \frac{k}{u_*^3}\left(\frac{\overline{wq^2}_{22.6}-\overline{wq^2}_{5.66}}{2\ln 4}\right), \tag{17}$$

which is equivalent to fitting a least squares linear function of ln$z$ to the data. The result was taken as the derivative at the midpoint of ln$z$, i.e., at 11.3 m. This procedure differs insignificantly from the alternative of fitting the data to z, not ln$z$, and assuming the approximation applies at 14 m, the midpoint in z.

The results (Fig. 2) show some evidence of obeying similarity, although the scatter is large. The turbulent transport as calculated from high-pass filtered (5-min running average removed)fluctuation data is also shown in Fig. 2. In general, the filtered results are slightly smaller but the scatter is not significantly different. Some of the scatter is probably due to the crude derivative approximation; had $\overline{wq^2}$ values been available at more levels, higher order least square curves could have been fitted to yield more accurate derivatives. Part of the scatter is probably also caused by the inherently

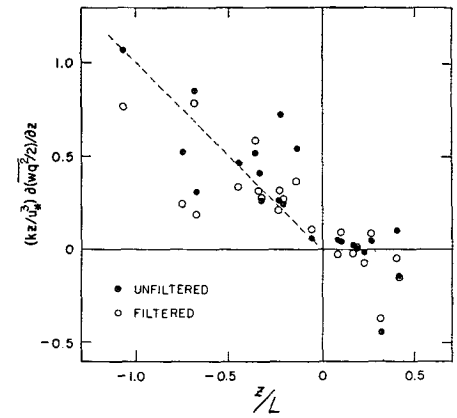

FIG. 2. Dimensionless rate of turbulent transport of energy calculated with and without a running-average filter on the velocity components.

larger uncertainty in third moments. To achieve the same accuracy, increasingly longer records are needed for higher moments (Lumley and Panofsky, 1964).

Turbulent transport can also be written as

$$\frac{kz}{2u_*^3}\frac{\partial\overline{wq^2}}{\partial z} = \frac{k}{2}\frac{\partial(\overline{wq^2}/u_*^3)}{\partial\ln(z/L)}. \tag{18}$$

The $\overline{wq^2}/u_*^3$ data show no trend with z/L under stable conditions, but the unstable side is shown in Fig. 3. The dashed curve is a reasonable fit to the data, and it together with Eq. (18) implies that turbulent transport follows the dashed line in Fig. 2. For $-1.0 \leqslant z/L \leqslant 0$ turbulent transport therefore behaves approximately as

$$\frac{kz}{2u_*^3}\frac{\partial\overline{wq^2}}{\partial z} \approx -\frac{z}{L}, \tag{19}$$

with an uncertainty of the order of ± 0.25.

The trend of the turbulent transport estimates on the stable side of Fig. 2 is less clear. While all but 2 of the 13 unstable runs had $\overline{wq^2}$ monotonically increasing with z,

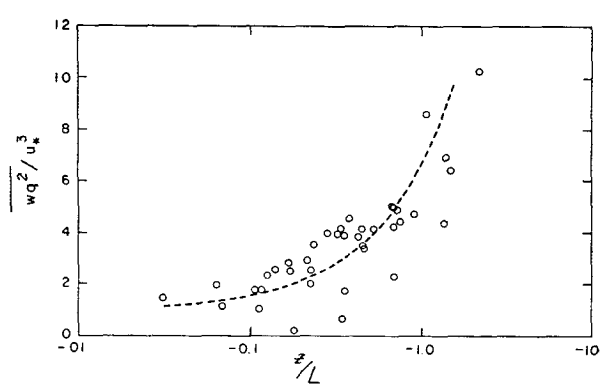

FIG. 3. Dimensionless turbulent energy flux under unstable conditions. Differentiation of the dashed curve gives the dashed line in Fig. 2.

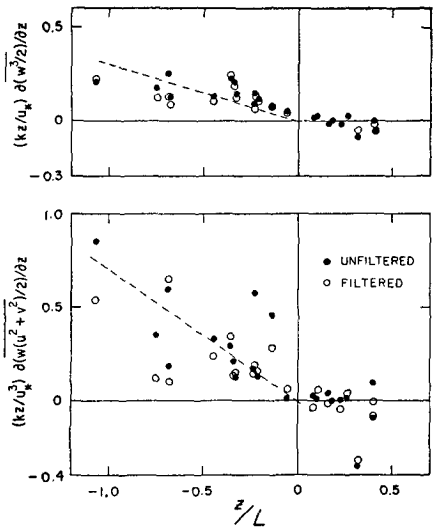

FIG. 4. Dimensionless rate of turbulent transport of vertical (upper figure) and horizontal (lower figure) components of energy, calculated with and without a running-average filter on the velocity components.

in almost all of the stable cases it was non-monotonic and had a maximum at 11.3 m. The transport rates in the layers between 5.66 and 11.3 m and between 11.3 and 22.6 m therefore tended toward losses and gains, respectively. This plot is not shown, but in similarity coordinates looks much like the stable side of Fig. 2; there is scatter about zero for small z/L and a tendency toward gains at larger z/L, but nearly all the estimates are smaller in magnitude than z/L. It appears, therefore, for $0 \leqslant z/L \leqslant 0.5$, that turbulent transport is quite small compared to the dominant terms in the energy budget.

The turbulent energy flux $\overline{wq^2}$ was positive in every unstable case. In conjunction with the result (19), this implies that energy is exported upward by turbulence at essentially the same rate it is produced by buoyancy. A flux divergence term represents transfer from one region in space to another, so that this exported energy has to appear as a local import, or gain, farther up. Recent measurements of Lenschow (1970) under unstable conditions and at heights of a few hundred meters do show a local gain, as expected.

A separation of turbulent transport into its contributions from horizontal and vertical energy components is shown in Fig. 4. The scatter is again rather large, but it appears that under unstable conditions roughly two-thirds of the transport is of the horizontal components.

d. Dissipation

The normalized dissipation results are shown in Fig. 5, in which each point represents a 1-hr run. The curve fitted through the unstable data has the form

$$\frac{kz\epsilon}{u_*^3}=(1+0.5|z/L|^{\frac{2}{3}})^{\frac{3}{2}}. \tag{20}$$

The curve has been assumed to go through 1.0 at the origin, in keeping with traditional thinking, but the data do not extend to sufficiently small z/L to test this point. Fig. 5 shows that dissipation exceeds the total production under moderately unstable conditions, with a balance being reached with increasing instability.

Under stable conditions, the dissipation data are fairly well represented by

$$\frac{kz\epsilon}{u_*^3}=[1+2.5(z/L)^{3/5}]^{3/2}. \tag{21}$$

The dissipation values and the measurement and analysis techniques which produced them were checked in three ways. First, as a check on the hot-wire performance, the values of $\overline{u^2}$ from hot wires and sonics were compared. Over 52 hr of data the values agreed within 4%. There was some run-to-run scatter, probably due to hot-wire drift, but the overall agreement is gratifying.

For the second check, the direct dissipation estimates were used to test the universality of the sonic anemometer velocity spectra in the inertial subrange. In large Reynolds number turbulence, it has been suggested (Lumley, 1967) that inertial subrange spectra depend in a universal way on local spectral flux. Spectral flux is the rate at which energy is transferred through the spectrum, from large scales to smaller ones, ultimately to be dissipated by viscosity at the smallest scales. In the absence of energy sources or drains, the spectral flux is simply the dissipation rate, and we have the Kolmogorov law for the inertial subrange. For the one-dimensional u spectrum this is

$$\left.\begin{aligned}\Phi_u(\kappa_1)&=\alpha_1\epsilon^{2/3}\kappa_1^{-5/3}\\ \int_0^\infty \Phi_u(\kappa_1)d\kappa_1&=\overline{u^2}\end{aligned}\right\}. \tag{22}$$

Previous measurements of the universal constant α_1

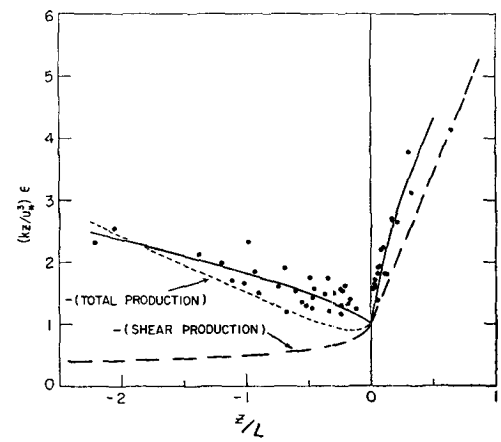

FIG. 5. Comparison of dimensionless rates of dissipation and production of energy.

from a wide variety of turbulent flows suggest that its value is ~ 0.5.

An extensive spectral analysis program is now underway, using the fast Fourier transform technique, and will be reported in detail later. For the present purposes, sonic anemometer u spectra were calculated for each of the 1-hr runs for which there also was a hot-wire dissipation value. The spectra were averaged over an hour and also over frequency bands, with the bandwidth limited by the requirement that the spectral distortion due to spectral curvature be negligible. The resulting spectra were very smooth, with typical scatter about the $-5/3$ power law behavior of no more than a few percent. Cospectra of Reynolds stress and heat flux in the spectral range considered (typically 0.5–5 Hz) were very small and falling faster than the velocity spectrum. In this range the change in spectral flux due to dissipation is negligible; the peak of the dissipation spectrum is at much higher frequencies, typically a few hundred hertz. If we assume that the effects of pressure and the third-moment terms are also small in this wavenumber range, the data meet the requirements for use in Eq. (22).

Taylor's hypothesis in the form $\kappa_1 = 2\pi f/U$ was used in conjunction with the measured ϵ values and Eq. (22) to derive estimates of α_1, with the results shown in Fig. 6. The mean value of α_1 is 0.52, with a standard deviation of 0.04.

These α_1 estimates are probably systematically high due to the effect of the fluctuating convection velocity on Taylor's hypothesis. Lumley's (1965) model shows that inertial subrange spectra, and therefore α_1 values, are overestimated by an amount depending on turbulence level. The correction is less than that already made to the dissipation rates, but shows that the average of 0.52 for α_1 is probably nearer 0.49.

Spectral analysis has also been carried out on selected hot-wire runs, giving an α_1 value of 0.53 ± 0.02 over a wide range of z/L values. The reduced standard deviation is a result of the more accurate calibration of the hot wires obtained by matching sonic and hot-wire inertial subrange spectral levels. It appears, therefore, that much of the scatter in the α_1 estimates of Fig. 6 is due to hot-wire drift. Considering the fluctuating convection velocity effect, the two α_1 values differ by about 10%, and if the larger value (which, corrected, is ~ 0.54) is correct, the dissipation data of Fig. 5 are about 15% high on the average, with the overestimate probably largest under stable conditions.

The third check involves the isotropy assumption inherent in the dissipation calculation. Isotropy also implies that the inertial subrange levels of the w and u spectra should be in a $\frac{4}{3}$ ratio; about 20 hr of sonic data from the upper two levels, with a stability range $-1.6 < z/L < 0.7$, were used to test this prediction. The average ratio was within a few percent of $\frac{4}{3}$ for this data, with a standard deviation of 0.06. For 10 hr of data from 5.66 m, the ratio averaged about 1.2, but it is possible

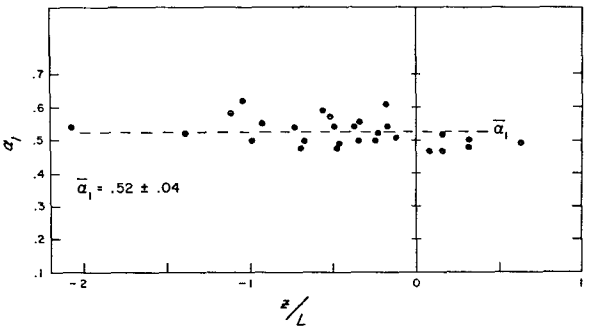

FIG. 6. Observations of the one-dimensional spectral constant.

that at higher frequencies the $\frac{4}{3}$ behavior exists. These results then give some justification for assuming isotropy in calculating dissipation.

e. The imbalance

Our results indicate that under unstable conditions, buoyant production and turbulent transport are approximately in balance, while under stable conditions turbulent transport is small. The budget therefore reduces to

$$\left.\begin{aligned} \overline{uw}\frac{\partial U}{\partial z} + \epsilon + I \approx 0, \quad & -1.0 \leqslant z/L \leqslant 0 \\ \frac{\partial}{\partial z}\overline{uw}\frac{\partial U}{\partial z} + \epsilon - \frac{g}{T}\overline{\theta w} + I \approx 0, \quad & 0 \leqslant z/L \leqslant 0.5 \end{aligned}\right\}, \tag{23}$$

where I is the imbalance. Our data show that under certain conditions the imbalance is substantial, and several factors arise as possible contributors.

First, it is recognized that any budget term found by difference contains the accumulated errors of the measured terms, which do show scatter about their fitted curves. Buoyant production, a second moment and a point measurement, shows the least scatter and is the most accurate. Turbulent transport, a spatial derivative of a third moment, shows the most scatter and its fitted curve is the least certain. While the use of fitted curves reduces the effects of random errors on the imbalance, residual systematic errors could be present. Broadly speaking, an overall accuracy figure of 15% is probably applicable, so that in the worst case, where errors are additive, the uncertainty in the imbalance could be appreciable.

This is probably the origin of a substantial part of the stable imbalance, which Eq. (23) shows to be a gain and about 30% of the dissipation rate. The stable dissipation rates, as mentioned earlier, could be 15% high; the transport data of Figs. 2 and 4 suggest that it could be a small gain; and the shear production rate of Eq. (15) could be slightly low. These errors could account for most of the imbalance under stable conditions.

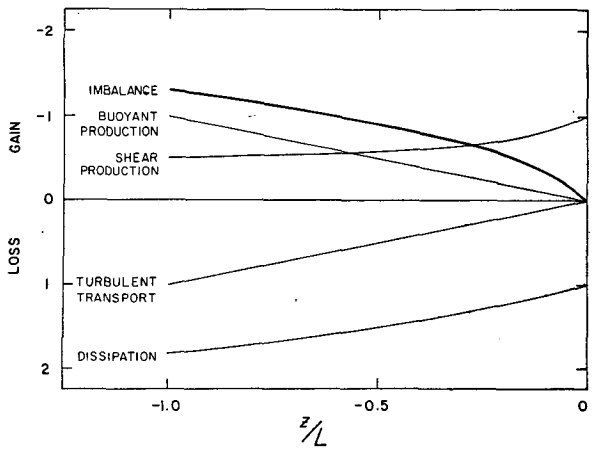

FIG. 7. Dimensionless energy budget under unstable conditions.

Under unstable conditions, however, the imbalance is considerably larger. Eqs. (14) and (20) for shear production and dissipation imply that the imbalance is

$$\frac{kz}{u_*^3}I=(1-15z/L)^{-\frac{1}{4}}-(1+0.5|z/L|^{\frac{2}{3}})^{\frac{3}{2}}. \tag{24}$$

Eq. (24) is plotted along with the measured terms in Fig. 7. At $z/L=-1.0$, the imbalance is about 75% of the dissipation rate and larger than any of the other terms; an explanation other than measurement error would seem to be needed to account for it.

A second possible contributor to the imbalance is horizontal inhomogeneity. If the mean flow depends on x as well as z, the energy budget has additional terms. The largest of these reflect additional production of energy and the advection of energy by the mean flow. If these are the cause of the imbalance, we have

$$\overline{u^2}\frac{\partial U}{\partial x}+\overline{w^2}\frac{\partial W}{\partial z}+\frac{U}{2}\frac{\partial\overline{q^2}}{\partial x}+\frac{W}{2}\frac{\partial\overline{q^2}}{\partial z}=I. \tag{25}$$

The mean continuity equation in the form

$$\frac{\partial U}{\partial x}+\frac{\partial W}{\partial z}=0, \tag{26}$$

and the assumption that $\partial U/\partial x$ is independent of z, give

$$(\overline{u^2}-\overline{w^2})\frac{\partial U}{\partial x}+\frac{U}{2}\frac{\partial\overline{q^2}}{\partial x}-\frac{z}{2}\frac{\partial U}{\partial x}\frac{\partial\overline{q^2}}{\partial z}=I. \tag{27}$$

Results of an analysis of the turbulent velocity variances, to be reported in detail in a forthcoming paper, are useful at this point. It is found that $\overline{q^2}$ varies sufficiently slowly with z in the surface layer under unstable conditions that the final term in (27) can be dropped in comparison with the first. Expressing the variances in terms of $\overline{q^2}$ then gives, at $z/L=-1.0$,

$$\frac{\overline{q^2}}{3}\frac{\partial U}{\partial x}+\frac{U}{2}\frac{\partial\overline{q^2}}{\partial x}=I\approx-1.3\frac{u_*^3}{kz}. \tag{28}$$

If, for example, two-thirds of the imbalance is due to the first term in Eq. (28), we can write the following expression for the required streamwise length scale of mean wind speed changes:

$$l_u=\frac{U}{\left|\frac{\partial U}{\partial x}\right|}\approx\frac{\overline{q^2}Ukz}{2.6u_*^3}. \tag{29}$$

If the second term in Eq. (28) causes essentially all the imbalance, the required length scale for streamwise changes in energy is found to be the same. At $z/L=-1.0$, $\overline{q^2}\approx 26u_*^2$, and with typical conditions of $U=500$ cm sec^{-1}, $u_*=30$ cm sec^{-1}, $z=10$ m, the scale is $\sim$600 m. This means that a mean wind speed decrease in the streamwise direction of 10% per 60 m would account for two-thirds of the observed energy budget imbalance at $z/L=-1.0$. The same rate of decrease of $\overline{q^2}$, on the other hand, would explain all of the imbalance.

The required gradients are severe, judging from the work of Dyer (1968) over apparently homogeneous terrain in Australia. He measured mean wind speed differences over horizontal separations of 200 m and found l_u values about 20 times greater than our calculations require.

The required inhomogeneity can also be compared with that expected due to normal boundary layer growth. The integrated form of the x-component equation of motion, neglecting pressure gradients and Coriolis forces and assuming two-dimensionality, is

$$\int_0^h\frac{\partial U}{\partial x}[U(h)-2U(z)]dz=\overline{uw}(h)+u_*^2. \tag{30}$$

If h is chosen as the height where stress vanishes, we have

$$\frac{\partial\tilde{U}}{\partial x}\tilde{U}h=-u_*^2, \tag{31}$$

where a tilde denotes a representative value for the layer. The scaling length for U is

$$|l_u|=\tilde{U}^2h/u_*^2\approx 8\times10^4\text{ m} \tag{32}$$

for typical conditions and h assumed conservatively to be only 300 m. This is more than two orders of magnitude greater than the required length scale, and it seems clear that any normal boundary layer growth had a negligible effect.

As mentioned earlier, the fetch for 2400 m was uniform wheat stubble; sections beyond this were in

varying crops, each with presumably different surface characteristics. This patchwork undoubtedly caused a complicated inhomogeneity in both u_*^2 and U, but judging from the boundary layer response calculations of Peterson (1969) the long uniform fetch would have reduced the inhomogeneity far below the level required to account for the imbalance.

The foregoing discussion has concerned what might be called large-scale inhomogeneity, since we interpreted the required $\partial U/\partial x$ in terms of a 10% change in U over 60 m. It is also equivalent to a 1% change over 6 m, and this type of small-scale inhomogeneity could have existed upwind of the tower. However, a turbulence element is swept through 6 m in a time short compared with typical turbulent time scales, so that we would not expect the turbulence *structure* to respond in such a short time, although its *intensity* would. If, for example, there is a small-scale inhomogeneity, the neglected terms in $\overline{u_i u_j}\partial U_i/\partial x_j$ would contribute to the energy budget locally, so the turbulence level leaving the region would be slightly different from that entering. This introduces a local advection term $U_i\partial(\overline{q^2}/2)/\partial x_i$ to cancel the additional production. The other terms in the budget, and their imbalance, are substantially unaffected by the inhomogeneity.

A third possible contributor to the energy budget imbalance is nonstationarity. If we attribute the imbalance to time changes in the turbulent energy, we find that the required time scale is, at $z/L=-1.0$,

$$\tau=\overline{q^2}\Big/\left|\frac{\partial\overline{q^2}}{\partial t}\right|\approx 3.5z/u_*. \tag{33}$$

At $z=10$ m and with $u_*=30$ cm sec^{-1}, $\tau\approx 2$ min; this means a rate of decrease of mean turbulence energy of 10% per 12 sec is required to account for the imbalance. Observation indicates that this rate is perhaps two orders of magnitude too high, so that we can eliminate nonstationarity from consideration.

Although little is known about the fourth possible contributor, pressure transport, there are bits of evidence that suggest it could be important. Batchelor (1951) used a simplified turbulence model to predict that the magnitudes of pressure and velocity fluctuations are related by

$$(\overline{p^2})^{\frac{1}{2}}\approx 0.2\rho\overline{q^2}. \tag{34}$$

Applying this to surface layer turbulence at $z/L=-1.0$ and taking the pressure-vertical velocity correlation coefficient as 0.5, we have

$$|\overline{pw}|\approx 5\rho u_*^3. \tag{35}$$

A vertical scaling length can be taken from the turbulent transport measurements. At $z/L=-1.0$, $\overline{wq^2}$ is typically $6u_*^3$ and the length is

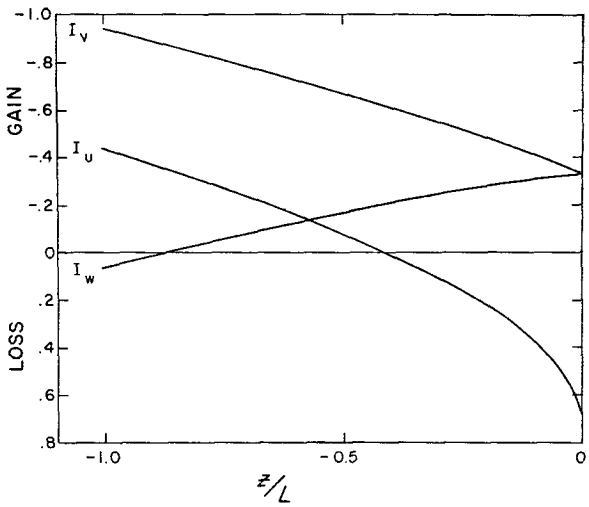

FIG. 8. Dimensionless components of the energy budget imbalance under unstable conditions.

$$l=\overline{wq^2}\Big/\left|\frac{\partial}{\partial z}\overline{wq^2}\right|\approx 2z. \tag{36}$$

If this is also the length scale for vertical variations in $\overline{pw}$, an estimate of pressure transport is

$$\left|\frac{1}{\rho}\frac{\partial\overline{pw}}{\partial z}\right|\approx\frac{1}{\rho}\frac{|\overline{pw}|}{l}\approx 0.9\frac{u_*^3}{kz}. \tag{37}$$

This is the same order of magnitude as the imbalance given by evaluating Eq. (24) at $z/L=-1.0$, i.e.,

$$I\approx -1.3u_*^3/(kz). \tag{38}$$

Kaimal and Businger (1970) recently analyzed the structure of a convective plume in some detail and found that the observed vertical accelerations could not be explained by the existing temperature gradient. They concluded that substantial vertical pressure gradients must exist to produce these accelerations.

Further evidence that fluctuating pressure fields can significantly influence turbulence dynamics under unstable conditions is given by the budget of $\overline{uw}$, also reported fully in a forthcoming publication. It is well known that pressure forces redistribute energy among components, and destroy $\overline{uw}$, in neutral boundary layers, and the measurements of the production and transport terms in the $\overline{uw}$ budget show that the rate at which stress is destroyed increases with instability. At $z/L=-1.0$, the results show that

$$\frac{1}{\rho}\overline{w\frac{\partial p}{\partial x}}+\frac{1}{\rho}\overline{u\frac{\partial p}{\partial z}}\approx -2.5\frac{u_*^3}{kz}, \tag{39}$$

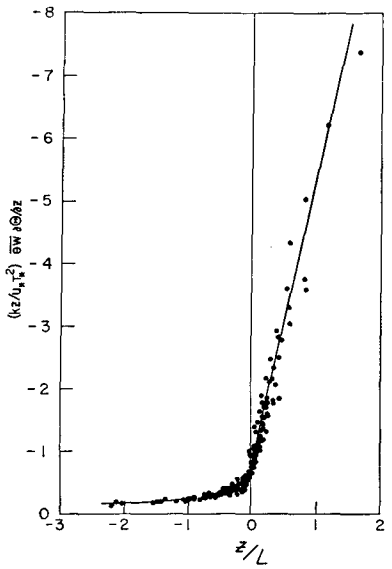

FIG. 9. Dimensionless rate of production of temperature variance.

which is the same order of magnitude as the energy budget imbalance.

A formal expression for pressure transport can be written, involving an integral of velocity-temperature and triple velocity correlations over the entire flow field. At this point, however, our knowledge of these correlations in the surface layer is so limited that it does not seem possible to make even a good approximation to the solution. Therefore, while it is clear that pressure fluctuations can be important in turbulence, it is still an open question whether they account for the imbalance of our energy budget under unstable conditions.

f. The imbalance components

It is interesting to consider the imbalance in the budgets of the energy components. These budgets are

$$\left.\begin{aligned} \frac{1}{2}\frac{\partial \overline{u^2}}{\partial t}+\overline{uw}\frac{\partial U}{\partial z}+\frac{1}{2}\frac{\partial \overline{wu^2}}{\partial z}+\frac{\epsilon}{3}+I_u=0 \\ \frac{1}{2}\frac{\partial \overline{v^2}}{\partial t}+\frac{1}{2}\frac{\partial \overline{wv^2}}{\partial z}+\frac{\epsilon}{3}+I_v=0 \\ \frac{1}{2}\frac{\partial \overline{w^2}}{\partial t}-\frac{g}{T}\overline{w\theta}+\frac{1}{2}\frac{\partial \overline{w^3}}{\partial z}+\frac{\epsilon}{3}+I_w=0 \end{aligned}\right\}. \tag{40}$$

The measurements indicate that turbulent transport is approximately equally divided among the three component energies. Knowing this and using the results for production and dissipation, we can solve Eqs. (40) for for the component imbalances. The results are shown in dimensionless form in Fig. 8.

It is generally accepted that the imbalances under neutral stability are caused by the pressure terms; this implies at $z/L=0$ that

$$\left.\begin{aligned} I_u=-\frac{1}{\rho}\overline{u\frac{\partial p}{\partial x}} \\ I_v=-\frac{1}{\rho}\overline{v\frac{\partial p}{\partial y}} \\ I_w=-\frac{1}{\rho}\overline{w\frac{\partial p}{\partial z}} \end{aligned}\right\}. \tag{41}$$

At neutral the imbalance components sum to zero, so that pressure forces simply transfer energy from $\overline{u^2}$ to the other components at equal rates without affecting the total energy. This transfer exists, of course, because at neutral the only energy source is shear production, but it produces only $\overline{u^2}$; pressure forces provide the necessary energy source for the other two components.

The behavior of the imbalance components changes drastically under unstable conditions, as shown in Fig. 8. The u component increases and is a gain at $z/L=-1.0$, while the w component decreases and is essentially zero at that point. The v imbalance remains a gain but steadily increases. At $z/L=-1.0$, therefore, the imbalance in the energy budget is essentially confined to the horizontal components. It follows that if pressure forces cause the large imbalance under unstable conditions, their input is largely received by u and v through accelerations caused by horizontal pressure gradients. It is interesting to note that in his study of the effects of heating on a laboratory boundary layer, Nicholl (1970) found evidence of significant pressure disturbances which he attributed to intense local convective activity. He suggested that the pressure gradients

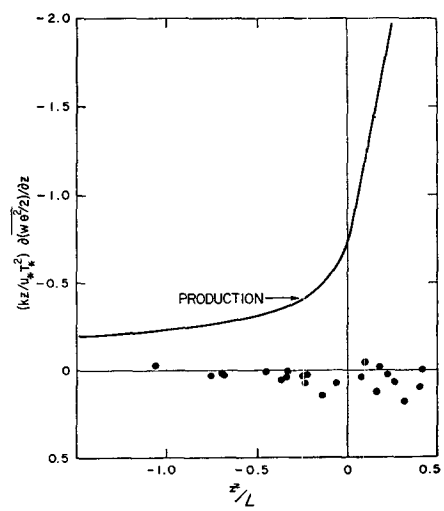

FIG. 10. Comparison of dimensionless rates of turbulent transport and production of temperature variance.

accelerated cooler air into the regions between the rising convective columns. Perhaps a similar situation exists in the unstable surface layer.

The proper interpretation of Fig. 8 is not entirely clear at this point, however. Fuller understanding may have to wait until a set of data including measurements of horizontal homogeneity are available, and perhaps until direct measurements of the pressure-velocity covariances have been made.

4. The temperature variance budget

The general form of the budget of temperature variance is (Lumley and Panofsky, 1964)

$$\frac{1}{2}\frac{\partial\overline{\theta^2}}{\partial t}+\frac{U_i}{2}\frac{\partial\overline{\theta^2}}{\partial x_i}+\overline{u_j\theta}\frac{\partial\Theta}{\partial x_j}+\frac{1}{2}\frac{\partial\overline{u_i\theta^2}}{\partial x_i}+D\overline{\frac{\partial\theta}{\partial x_i}\frac{\partial\theta}{\partial x_i}}=0. \quad (42)$$

Eq. (42) is actually the budget of $\overline{\theta^2}/2$; the factor $\frac{1}{2}$ is included for consistency with the energy budget. Under stationary, horizontally homogeneous conditions, Eq. (42) simplifies to

$$\overline{w\theta}\frac{\partial\Theta}{\partial z}+\frac{1}{2}\frac{\partial\overline{w\theta^2}}{\partial z}+D\overline{\frac{\partial\theta}{\partial x_i}\frac{\partial\theta}{\partial x_i}}=0. \quad (43)$$

The first term in Eq. (43) is the rate of production by the interaction of vertical heat flux and vertical mean temperature gradient; we call this production. The second term represents the divergence of the turbulent flux of temperature variance, or simply turbulent transport. The final term is the rate of destruction of fluctuations by smoothing due to the molecular diffusivity D, or the temperature dissipation rate. For consistency with previous work, we label the dissipation term N; the symbol χ is often used for the dissipation term in the budget of $\overline{\theta^2}$, and $\chi=2N$.

We can nondimensionalize the budget with u_*, z and a temperature scale T_*, defined by

$$T_*=-\overline{w\theta}/u_*, \quad (44)$$

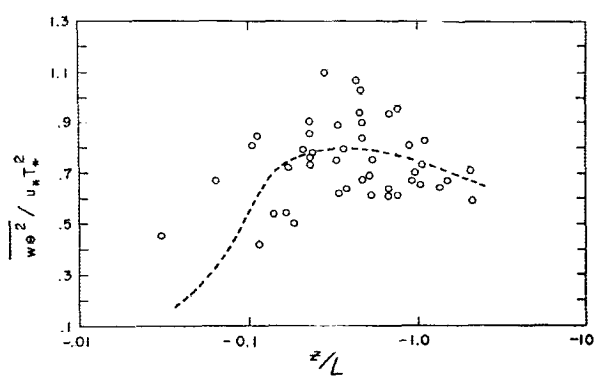

FIG. 11. Dimensionless temperature variance flux under unstable conditions. Differentiation of the dashed curve gives the dashed curve in Fig. 12.

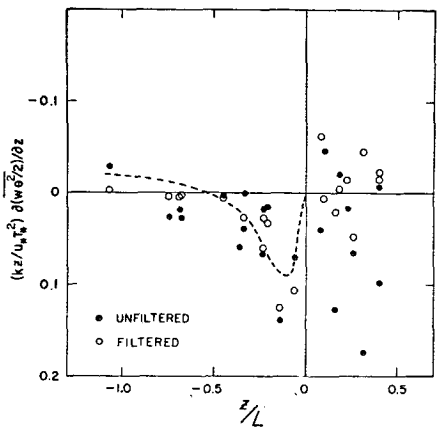

FIG. 12. Dimensionless rate of turbulent transport of temperature variance, calculated with and without a running-average filter on the vertical velocity and temperature fluctuations.

and we note that T_* is independent of height in the surface layer. It is convenient to include von Kármán's constant k in the normalization, so that production becomes

$$\frac{kz}{u_*T_*^2}\overline{w\theta}\frac{\partial\Theta}{\partial z}=-\frac{kz}{T_*}\frac{\partial\Theta}{\partial z}=-\phi_h, \quad (45)$$

or simply the nondimensional temperature gradient. The analysis of the profiles from this experiment shows that under unstable conditions, the formula

$$\phi_h=0.74(1-9z/L)^{-\frac{1}{2}} \quad (46)$$

fits the data well. Under stable conditions, the data follow

$$\phi_h=0.74+4.7z/L. \quad (47)$$

These interpolation formulas are shown with the data in Fig. 9.

The turbulent transport was calculated with the same three-point approximation used in the energy budget, with the results shown in Fig. 10. Again, the transport term can also be written as

$$\frac{kz}{2u_*T_*^2}\frac{\partial\overline{w\theta^2}}{\partial z}=-\frac{k}{2}\frac{\partial(\overline{w\theta^2}/u_*T_*^2)}{\partial\ln(z/L)}, \quad (48)$$

which suggests another way of estimating this term. The stable values of $\overline{w\theta^2}/(u_*T_*^2)$ show no evidence of a trend with z/L, but similarity is followed fairly well under unstable conditions, as shown in Fig. 11. The dashed curve in Fig. 11 corresponds, through Eq. (48), to the dashed curve in Fig. 12, and suggests that the transport term is about an order of magnitude smaller than production. The trend of the dashed curve should perhaps not be taken too seriously because of the scatter in the data on which it is based, but there is a hint that transport changes sign and becomes a gain under very unstable conditions. This is consistent with observations (Deardorff, 1966) that under very unstable con-

ditions a positive heat flux can exist in the presence of a vanishing or counter-gradient of potential temperature ($\partial\Theta/\partial z \geqslant 0$). In this case the temperature variance production term vanishes or becomes a loss, and another mechanism is needed to maintain the temperature fluctuations. Deardorff suggested that the turbulent transport term takes over this role, giving support to the trend in Fig. 12 under very unstable conditions.

An analysis of the effects of horizontal inhomogeneity shows that under typical conditions a mean temperature variation with x of 10C per 100 m, or a temperature variance change of 10% per 10 m, would be required to balance the production rate of temperature variance. These rates of change are far greater than expected over the site. Since nonstationarity also cannot contribute significantly, the form (43) of the budget can be taken as a reasonable approximation, with the imbalance between production and turbulent transport a measure of the temperature dissipation rate N.

The temperature dissipation rates derived in this manner were used in conjunction with inertial subrange temperature spectra to obtain estimates for the spectral constant β_1. In this interval the temperature spectrum has the form

$$\left.\begin{aligned}\Phi_T(\kappa_1) &= \beta_1 \epsilon^{-1/3} N \kappa_1^{-5/3} \\ \overline{\theta^2} &= \int_0^\infty \Phi_T(\kappa_1)\, d\kappa_1\end{aligned}\right\}. \tag{49}$$

There were 27 one-hour runs for which there were direct ϵ measurements and temperature spectra. With the approximation $N = -\overline{\theta w}\partial\Theta/\partial z$, the $-5/3$ ranges (generally in the band 0.5–5 Hz) of the spectra were used to derive β_1 estimates. The averages of the 27 estimates was 0.79 with a standard deviation of 0.10.

This β_1 value is in general agreement with earlier results. Grant *et al.* (1968) found 0.62 in the ocean; Gibson and Schwarz (1963) report 0.70 in laboratory turbulence; and Panofsky (1969) cites a Russian survey which gives values in the range of 0.41–0.88. The large scatter in these estimates is perhaps partly due to the greater difficulty in directly measuring β_1 compared to α_1. In addition, many of the meteorological observations of β_1 are indirect, involving dissipation rates inferred from measurements of fluxes, profiles, or other quantities. Such a scheme then requires knowledge of similarity relations or universal constants; the problem is that, generally speaking, the latter are far from well-established.

5. Conclusions

The turbulent energy budget in the surface layer appears to follow Obukhov similarity quite well. The relative importance of the various terms in the budget depends on stability. Under stable conditions, in the range $0<z/L<0.5$, shear production and viscous dissipation are the dominant terms and are essentially in balance. The buoyant term is a small loss, and turbulent transport is also very small. Under unstable conditions, $-1.0<z/L<0$, all four measured terms are significant. Shear production gradually becomes less important as instability increases, and buoyant production assumes a dominant role as the energy source. Viscous dissipation approximately balances the sum of these two production terms. In addition, energy is lost at a rate increasing with instability, due to vertical export by the turbulence.

Under very unstable conditions the four measured terms are far out of balance, and the accuracy is felt to be sufficient to justify taking the trend of the imbalance as real.

The unmeasured terms, those reflecting possible horizontal inhomogeneity and pressure transport, would naturally be suspected of causing the imbalance. However, calculations show that very strong horizontal gradients are required to explain the imbalance, and it would be surprising if such inhomogeneity could exist over the long uniform fetch of the site. Very little is known about pressure transport, but what little information we have does not rule out its being important under unstable conditions.

The production rate of temperature variance, $-\phi_h$, also follows similarity very well in the surface layer. It exceeds the vertical turbulent transport term by an order of magnitude in the range $-1.0<z/L<0.5$, which implies that to a good approximation the production and molecular dissipation rates of temperature variance are equal. The estimates of the universal spectral constants, made with the direct dissipation measurements, are in general agreement with other observations. The α_1 value was near 0.5, while the temperature constant β_1 averaged 0.8.

Acknowledgments. This paper was made possible through the efforts of all the members of the Boundary Layer Branch of AFCRL, who carried out the field experiments and helped in the data processing. We are particularly grateful for the efforts of Mrs. J. O'Donnell in computer programming and Miss S. Tourville in typing the manuscript. Drs. Niels E. Busch, Duane A. Haugen and J. Chandron Kaimal made several helpful comments on the manuscript for which we are most grateful.

REFERENCES

Batchelor, G. K., 1951: Pressure fluctuations in isotropic turbulence. *Proc. Cambridge Phil. Soc.*, **47**, 359–374.

Businger, J. A., J. C. Wyngaard, Y. Izumi and E. F. Bradley, 1971: Flux-profile relationships in the atmospheric surface layer. *J. Atmos. Sci.*, **28**, 181–189.

Deardorff, J. W., 1966: The counter-gradient heat flux in the lower atmosphere and in the laboratory. *J. Atmos. Sci.*, **23**, 503–506.

Dyer, A. J., 1968: An evaluation of eddy flux variation in the atmospheric boundary layer. *J. Appl. Meteor.*, **7**, 845–850.

Gibson, C. H., and W. H. Schwarz, 1963: The universal equilibrium spectra of turbulent velocity and scalar fields. *J. Fluid Mech.*, **16**, 365–384.

Grant, H. L., B. A. Hughes, W. M. Vogel and A. Moilliet, 1968: The spectrum of temperature fluctuations in turbulent flow. *J. Fluid Mech.*, **34**, 423–442.

Haugen, D. A., J. C. Kaimal and E. F. Bradley, 1971: An experimental study of Reynolds stress and heat flux in the atmospheric surface layer. *Quart. J. Roy. Meteor. Soc.* (in press).

Heskestad, G., 1965: A generalized Taylor's hypothesis with application for high Reynolds number turbulent shear flows. *J. Appl. Mech.*, **87**, 735–739.

Izumi, Y., and M. L. Barad, 1970: Wind speeds as measured by cup and sonic anemometers and influenced by tower structure. *J. Appl. Meteor.*, **9**, 851–856.

Kaimal, J. C., and J. A. Businger, 1970: Case studies of a convective plume and a dust devil. *J. Appl. Meteor.*, **9**, 612–620.

——, D. A. Haugen and J. T. Newman, 1966: A computer-controlled mobile micrometeorological observation system. *J. Appl. Meteor.*, **5**, 411–420.

Lenschow, D. H., 1970: Airplane measurements of planetary boundary layer structure, *J. Appl. Meteor.*, **9**, 874–884.

Lumley, J. L., 1965: Interpretation of time spectra measured in high-intensity shear flows. *Phys. Fluids*, **8**, 1056–1062.

——, 1967: Similarity and the turbulent energy spectrum. *Phys. Fluids*, **10**, 855–858.

——, and H. A. Panofsky, 1964: *The Structure of Atmospheric Turbulence.* New York, Interscience, 239 pp.

Monin, A. S., and A. M. Obukhov, 1954: Basic laws of turbulent mixing in the ground layer of the atmosphere. *Tr. Geofiz. Inst. Akad. Nauk SSSR*, **151**, 163–187.

Nicholl, C. I. H., 1970: Some dynamical effects of heat on a turbulent boundary layer. *J. Fluid Mech.*, **40**, 361–384.

Obukhov, A. M., 1946: Turbulence in an atmosphere with inhomogeneous temperature. *Tr. Inst. Teoret. Geofiz. Akad. Nauk SSSR*, **1**, 95–115.

Panofsky, H. A., 1969: The spectrum of temperature. *Radio Sci.*, **4**, 1143–1146.

Peterson, E. W., 1969: Modification of mean flow and turbulent energy by a change in surface roughness under conditions of neutral stability. *Quart. J. Roy. Meteor. Soc.*, **95**, 561–575.

Rose, W. G., 1962: Some corrections to the linearized response of a constant temperature hot-wire anemometer operated in a low-speed flow. *J. Appl. Mech.*, **29**, 554–558.

Wyngaard, J. C., 1969: Spatial resolution of the vorticity meter and other hot-wire arrays. *J. Sci. Instr.*, **2**, 983–987.

——, and J. L. Lumley, 1967: A sharp cut-off spectral differentiator. *J. Appl. Meteor.*, **6**, 952–955.